IEEE Access
Multidisciplinary | Rapid Review | Open Access Journal

Received June 8, 2020, accepted June 14, 2020, date of publication June 17, 2020, date of current version June 26, 2020.

Digital Object Identifier 10.1109/ACCESS.2020.3003028

Security-Enhanced 3D-CAP-PON Based on Two-Stage Spherical Constellation Masking

JIANXIN REN[1], BO LIU[2], XIANGYU WU[1], XING XU[1], YAYA MAO[2], YONGFENG WU[2], XIUMIN SONG[1], LEI JIANG[2], JINGYI ZHANG[2], YING ZHANG[3], AND XIANGJUN XIN[1]

[1]Beijing Key Laboratory of Space-Ground Interconnection and Convergence, School of Electronic Engineering, Beijing University of Posts and Telecommunications, Beijing 100876, China
[2]Institute of Optics and Electronics, Nanjing University of Information Science and Technology, Nanjing 210044, China
[3]State Key Laboratory of Advanced Optical Communication Systems and Networks, Department of Electronics, School of Electronics Engineering and Computer Science, Peking University, Beijing 100871, China

Corresponding author: Bo Liu (bo@nuist.edu.cn)

This work was supported in part by the National Key Research and Development Program of China under Grant 2018YFB1800901, in part by the National Natural Science Foundation of China under Grant 61835005, Grant 61822507, Grant 61522501, Grant 61475024, Grant 61675004, Grant 61705107, Grant 61727817, Grant 61775098, Grant 61720106015, Grant 61875248, and Grant 61975084, in part by the Beijing Young Talent under Grant 2016000026833ZK15, in part by the BUPT Excellent Ph.D. Students Foundation under Grant CX2020301, in part by the Open Fund of IPOC (BUPT), in part by the Jiangsu Talent of Innovation and Entrepreneurship, and in part by the Jiangsu Team of Innovation and Entrepreneurship.

ABSTRACT A security-enhanced three-dimensional carrier-less amplitude phase passive optical network (3D-CAP-PON) based on two-stage spherical constellation masking is proposed in this paper, where Chua's circuit map and one-dimensional Logistic map are jointly applied to implement rotation-based and scaling-based 3D-constellation masking. The rotation masking converts the constellation into two spherical layers with different radii, while the scaling masking leads to a hollow sphere with thick wall. The dimensional expansion of the constellation, combined with the joint adoption of two chaotic models, enable more flexibility and security for constellation encryption. And the key space of the proposed scheme is 1.2×10^{73} when taking only initial values and step lengths of chaotic models into consideration. A 4 Gb/s encrypted 3D-CAP-16 signal transmission over 25 km standard single mode fiber (SSMF) is experimentally demonstrated. The experimental results indicate that the proposed scheme can effectively protect the system from any illegal optical network unit (ONU) attack, proving to be a promising candidate for future physically secure 3D-CAP-PON.

INDEX TERMS 3D constellation, spherical constellation masking, chaotic encryption, carrier-less amplitude phase, passive optical network.

I. INTRODUCTION

With the rapid increase of broadband services demands, passive optical network (PON), standing out as an effective and future-proof network architecture due to its lower power consumption, higher data transmission rate and wider converge, has been attracting much attention for next-generation (NG) access system [1]–[4]. Meanwhile, carrier-less amplitude phase (CAP) modulation is capable of achieving orthogonal multiplexing on the basis of signal pulse shaping and matched filtering without extra expensive radio frequency sources and mixers. By applying the multi-dimensional CAP technique to PON system, the flexibility can be enhanced to provide differentiated services to various subscribers with a finer granularity [5]–[9]. These huge advantages have enabled CAP technique to gain more and more momentum in the low-cost and high-speed PON. However, the broadcasting mechanism in the PON, where downstream signal is transmitted to the different optical network units (ONUs) in a broadcasting manner, has inadvertently made it possible for the illegal users to easily tap into the downstream signals. Therefore, the security of the CAP-PON system must be taken into serious consideration [10], [11].

There have been many proposals regarding the secure communication in the physical or even upper layers currently. Due to the unprotected control data or headers in the upper layers encryption, it is vulnerable to attacks against the lowest layer [12], [13]. Compared with the upper layers

The associate editor coordinating the review of this manuscript and approving it for publication was Jinming Wen.

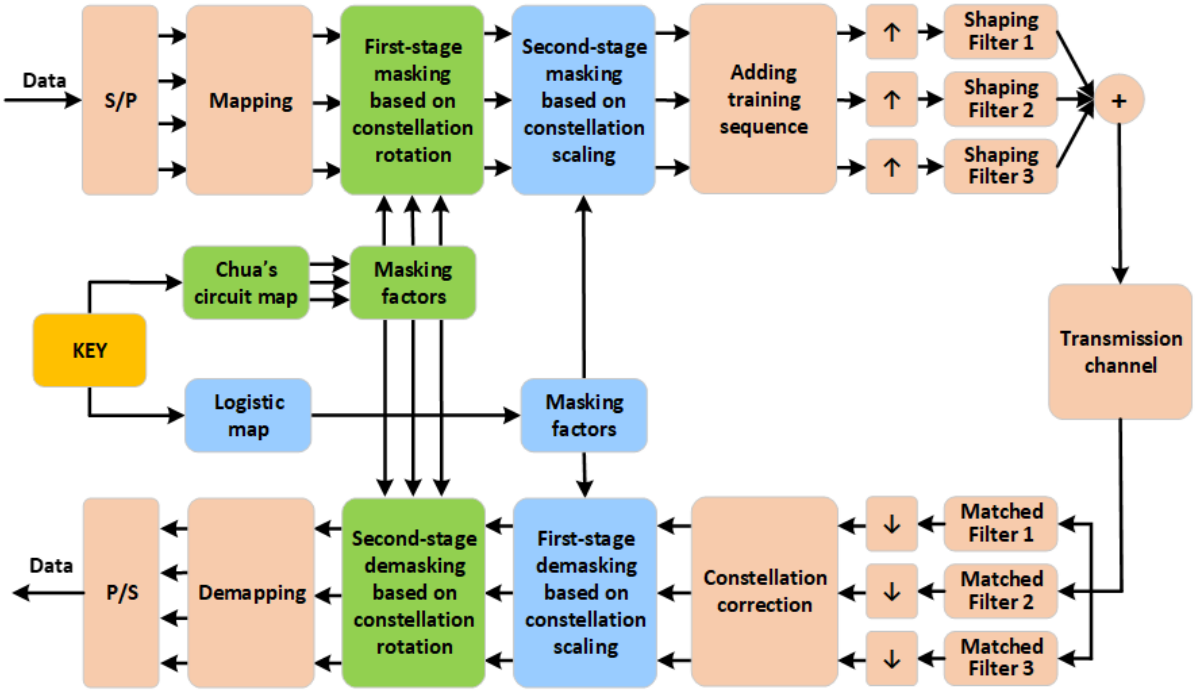

FIGURE 1. Schematic of the proposed security-enhanced 3D-CAP-PON based on two-stage spherical constellation masking.

encryption, the physical layer encryption based on efficient and convenient digital signal processing (DSP) technique can fundamentally protect the high-speed transmitted data from any malicious attack. Wherein chaotic encryption has played an important role, given its superiority of ergodicity, pseudo-randomness and the sensitivity to initial values and control parameters. So far there have been quite a few investigations of chaotic encryption in the constellation mapping, including constellation masking [14], [15], chaotic constellation transformation [16], chaotic active constellation extension [17], and noise-like constellation mapping [18]. These schemes are encrypting constellation either by randomly rotating and moving or by swapping the constellation points, so as to achieve the security communication in the physical layer. However, these encryption methods are mostly operated in a two-dimensional constellation with few studies done in terms of three-dimensional constellation. The constellation encryption in the lower dimension often limits the flexibility of the constellation transformation and masking, thereby dampening the security performance of the constellation encryption to a certain extent.

In this paper, we propose and demonstrate a security-enhanced 3D-CAP-PON based on two-stage spherical constellation masking, in which Chua's circuit map and one-dimensional Logistic map are adopted as chaotic models to generate masking factors for 3D constellation rotating and scaling respectively. The rotation masking converts the constellation into two spherical layers with different radii, while the scaling masking leads to a hollow sphere with thick wall. Based on these two chaotic models, the joint masking of constellation rotating and scaling in 3D-CAP-PON is implemented. Dimensional expansion can bring about more flexibility for the transformation and masking of the constellation, as well as the security performance enhancement for the constellation encryption. Moreover, the extension of the minimum Euclidean distance between constellation points in three-dimensional space can improve the bit error rate (BER) performance and enable better signal quality to a certain extent. The feasibility of the proposed scheme is successfully verified by an experiment of 4 Gb/s encrypted 3D-CAP-16 signal transmission over 25 km standard single mode fiber (SSMF).

II. PRINCIPLE OF SECURITY-ENHANCED 3D-CAP-PON BASED ON TWO-STAGE SPHERICAL CONSTELLATION MASKING

Figure 1 depicts the principle of proposed security-enhanced 3D-CAP-PON based on two-stage spherical constellation masking. Taking 16-ary 3D constellation for illustration, the 3D constellation composed of four regular tetrahedrons is formed after serial-to-parallel (S/P) converting and constellation mapping, as shown in Fig. 2(a) [19]. It can be seen that the minimum Euclidean distance between constellation points is set as 2, with 4 constellation points located in the inner layer and 12 constellation points located in the outer layer. The detailed mapping rule is demonstrated in Table 1. Then two-stage spherical constellation masking is performed for constellation rotation and scaling based on Chua's circuit map and one-dimensional Logistic map respectively, where KEY includes the initial values, control parameters and step

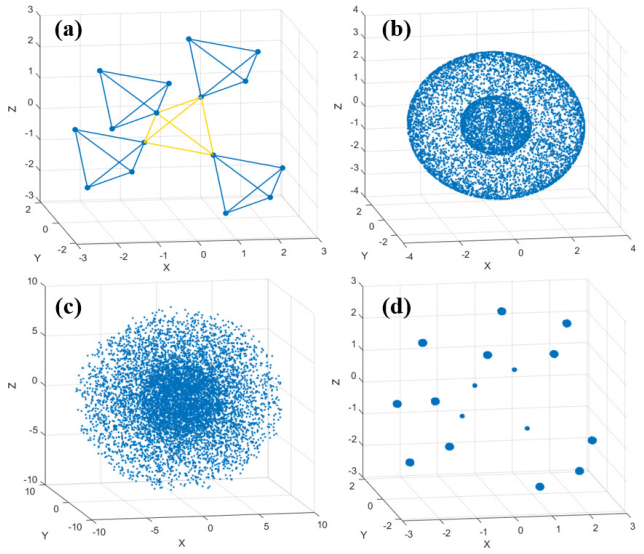

FIGURE 2. Constellation diagrams (a) before masking, (b) after first-stage masking based on constellation rotation, (c) after second-stage masking based on constellation scaling, (d) with correct demasking.

lengths of the chaotic models. The diversity of the secret key parameters in these two chaotic models can effectively guarantee and enhance physical layer security. In addition, to counteract the impact of transmission channel on the constellation rotating and scaling, the training sequence is added right after the masked data, so that channel compensation can be conducted before the constellation decryption at the receiver. Finally, the 3D-CAP signal is sent for transmission after up-sampling, shaped filtering and addition. At the receiver, the inverse procedures as opposed to the one at the transmitter are carried out to demodulate and decrypt the received signal.

To be specific, in the first-stage masking based on constellation rotation, Chua's circuit map is adopted as the chaotic model, which can be expressed as follows [20]:

$$\begin{cases} \partial l/\partial t = a\left(m - l - f\left(l\right)\right) \\ \partial m/\partial t = l - m + n \\ \partial n/\partial t = -bm, \end{cases}$$
$$f\left(l\right) = dl + 0.5\left(c - d\right)\left(\left|l + 1\right| - \left|l - 1\right|\right), \qquad (1)$$

where a, b, c and d are set as constants with values of 10, 14.87, -1.27 and -0.65, respectively. At this moment, the chaotic system is in a state of chaos. l, m and n are set as variables with the range of $(-3, 3)$, $(-1, 1)$ and $(-5, 5)$, respectively. t is a variable positive step length. And the 4^{th} Runge-kutta method is performed to solve the partial differential equation in (1). In this paper, the initial values of $\{l_0, m_0, n_0\}$ are set as $\{0.2, -0.1, 0.2\}$, and the corresponding phase diagram of Chua's circuit map is shown in Fig. 3(a). The phase diagrams in phase planes $(m - n)$, $(l - m)$, and $(l - n)$ are shown in Fig. 3(b), (c), and (d), respectively. It can be seen that not only is Chua's circuit map easy to implement, but it can exhibit complex dynamics of bifurcation and chaos with high security performance. This chaotic model can simultaneously generate three chaotic sequences of $\{l, m, n\}$ with varying ranges of numerical values. Therefore, the fractional parts of these three sequences are chosen to generate masking factors, that is, the three angles ρ_{i1}, ρ_{i2}, ρ_{i3} of constellation rotating counterclockwise around the axes of X, Y and Z. The specific rules are as follows:

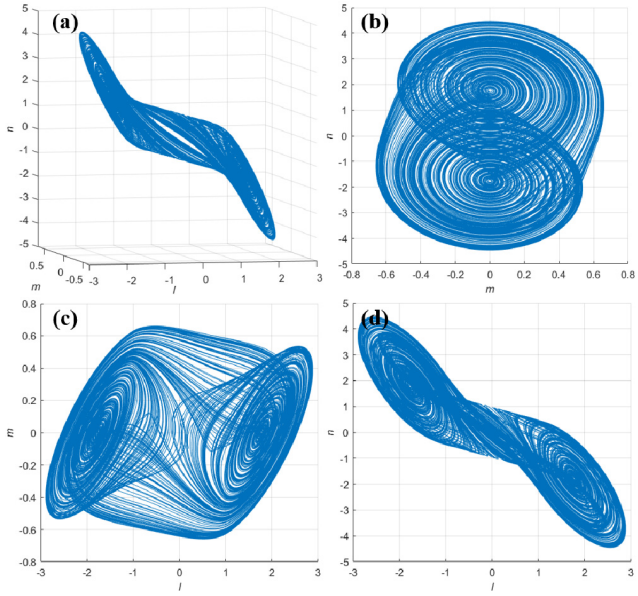

FIGURE 3. Phase diagram of Chua's circuit map.

$$\begin{cases} \rho_{i1} = floor\left(\mathrm{mod}\left(l \cdot 10^7, 360\right)\right) \\ \rho_{i2} = floor\left(\mathrm{mod}\left(m \cdot 10^7, 360\right)\right) \\ \rho_{i3} = floor\left(\mathrm{mod}\left(n \cdot 10^7, 360\right)\right). \end{cases} \qquad (2)$$

As is processed in (2), three rotating angles ρ_{i1}, ρ_{i2}, ρ_{i3} in the range of (0, 360) can be acquired, with which the constellation points in the 3D space are counterclockwise rotated around the axes of X, Y and Z, so that the first-stage masking based on constellation rotation is implemented. As such, the new coordinate for a certain constellation point C_i of $C_i = (C_{i1}, C_{i2}, C_{i3})^T$ after three rotations can be expressed as:

$$C_i' = \begin{pmatrix} C_{i1}' \\ C_{i2}' \\ C_{i3}' \end{pmatrix} = \begin{pmatrix} 1 & 0 & 0 \\ 0 & \cos\rho_{i1} & -\sin\rho_{i1} \\ 0 & \sin\rho_{i1} & \cos\rho_{i1} \end{pmatrix} C_i, \qquad (3)$$

$$C_i'' = \begin{pmatrix} C_{i1}'' \\ C_{i2}'' \\ C_{i3}'' \end{pmatrix} = \begin{pmatrix} \cos\rho_{i2} & 0 & -\sin\rho_{i2} \\ 0 & 1 & 0 \\ \sin\rho_{i2} & 0 & \cos\rho_{i2} \end{pmatrix} C_i', \qquad (4)$$

$$C_i''' = \begin{pmatrix} C_{i1}''' \\ C_{i2}''' \\ C_{i3}''' \end{pmatrix} = \begin{pmatrix} \cos\rho_{i3} & -\sin\rho_{i3} & 0 \\ \sin\rho_{i3} & \cos\rho_{i3} & 0 \\ 0 & 0 & 1 \end{pmatrix} C_i''. \qquad (5)$$

where C_i', C_i'', C_i''' denote the coordinates of the constellation point while rotating around the axes of X, Y and Z, respectively. The constellation diagram after the first-stage masking based on constellation rotation is displayed in Fig. 2(b), where two spherical layers with different radii can be observed.

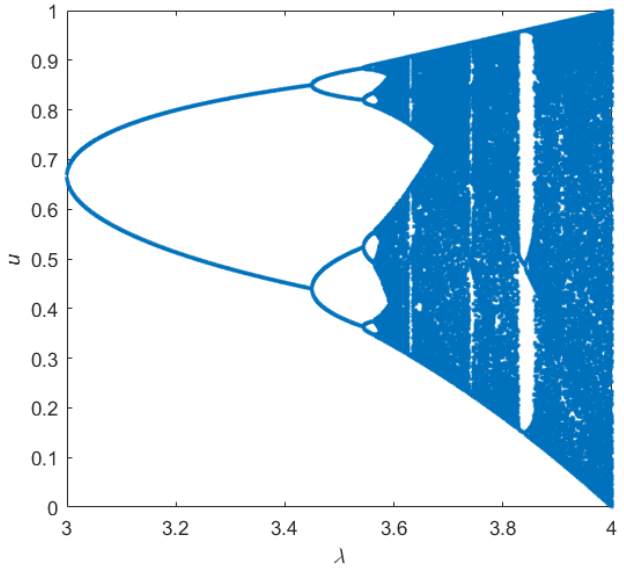

FIGURE 4. The bifurcation diagram of one-dimensional Logistic map.

In the second-stage masking based on constellation scaling, one-dimensional Logistic map is considered to generate related masking factors, which is given by [21]:

$$u_{n+1} = \lambda u_n (1 - u_n), \quad u \in (0, 1), \tag{6}$$

where λ represents the bifurcation parameter with the range of $[1, 4]$, u_0 can be any arbitrary value in the range of $(0, 1)$ and u_n is the nth value iterated by (6). Once the bifurcation parameter λ is determined, the Logistic map can iterate a unique sequence for any initial value of u_0. Any tiny movement of u_0 can lead to significant discrepancy with regarding to the generated sequence. Figure 4 shows the bifurcation diagram of the Logistic map, where initial value of u_0 is set as 0.37259. It can be seen that as λ exceeds 3.569945672, the sequence will fall into chaos. Taking this into consideration, λ is set as 3.95 in this paper. And the fractional part of u is selected to determine the masking factor in the process of constellation scaling. Since the scaling down for the inwards convergence of the constellation makes it hard for the receiver to judge and determine the constellation points, only 1 to 3 times of random scaling up is performed on the 3D constellation. Detailed rule for the generation of masking factor is shown as follows:

$$\omega_i = floor\left(\mathrm{mod}\left(u \cdot 10^7, 100\right)\right)/100 \times 2 + 1, \tag{7}$$

As is processed in (7), the constellation scaling factor in the range of [1, 3] can be obtained, based on which second-stage constellation masking is performed to determine the coordinate of constellation point C_i'''' given as follow:

$$C_i'''' = \begin{pmatrix} C_{i1}'''' \\ C_{i2}'''' \\ C_{i3}'''' \end{pmatrix} = \omega_i \cdot C_i'''. \tag{8}$$

The constellation diagram after the second-stage masking based on constellation scaling is illustrated in Fig. 2(c), where two spherical layers with different radii are converted to a hollow sphere with thick wall.

Based on these two different chaotic models, constellation rotation and scaling are performed to implement two-stage masking, which can increase the number of parameters in the KEY to significantly raise more difficulties for illegal ONU to access transmitted information. At the receiver, illegal ONU in absence of correct secret key is having little possibility to recover the original constellation for information stealing. While ONU granted with the correct secret key can inevitably obtain the original constellation after proper decryption, as shown in Fig. 2(d).

TABLE 1. 16-ary 3D constellation mapping rule.

Bits	Constellation points	Bits	Constellation points
1101	(0.7071,0.7071,0.7071)	1100	(0.7071,2.1213,2.1213)
1000	(2.1213,2.1213,0.7071)	1001	(2.1213,0.7071,2.1213)
1111	(0.7071,-0.7071,-0.7071)	1110	(0.7071,-2.1213,-2.1213)
1010	(2.1213,-2.1213,-0.7071)	1011	(2.1213,-0.7071,-2.1213)
0101	(-0.7071,0.7071,-0.7071)	0100	(-0.7071,2.1213,-2.1213)
0000	(-2.1213,2.1213,-0.7071)	0001	(-2.1213,0.7071,-2.1213)
0111	(-0.7071,-0.7071,0.7071)	0110	(-0.7071,-2.1213,2.1213)
0010	(-2.1213,-2.1213,0.7071)	0011	(-2.1213,-0.7071,2.1213)

III. EXPERIMENT AND RESULTS

To verify the performance of the proposed physical layer encryption scheme, an experiment is carried out as shown in Fig. 5. At the optical line terminal (OLT), offline DSP is performed to implement 3D-CAP modulation and data encryption based on two-stage spherical constellation masking for the original data. The up-sampling factor in 3D-CAP modulation is set as 11, the same as the tap number of the shaping filters. And an arbitrary waveform generator (AWG, TekAWG70002A) with the maximum sampling rate of 25 GSa/s is used to perform digital-to-analog conversion for the encrypted 3D-CAP signal. Following the linear amplification by an electrical amplifier (EA), the encrypted electrical 3D-CAP signal is injected into the Mach-Zehnder modulator (MZM) for intensity modulation to generate modulated optical signal, which is then transmitted over a 25 km SSMF. In the experiment, a continuous wave (CW) laser with the operating wavelength of 1550 nm and optical power of 10 dBm serves as the light source. At the ONU, a variable optical attenuator (VOA) is put in place to adjust the received optical power for the optical signal detection and conversion by a photodiode (PD) with bandwidth of 40 GHz. And after the analog-to-digital conversion for the encrypted electrical

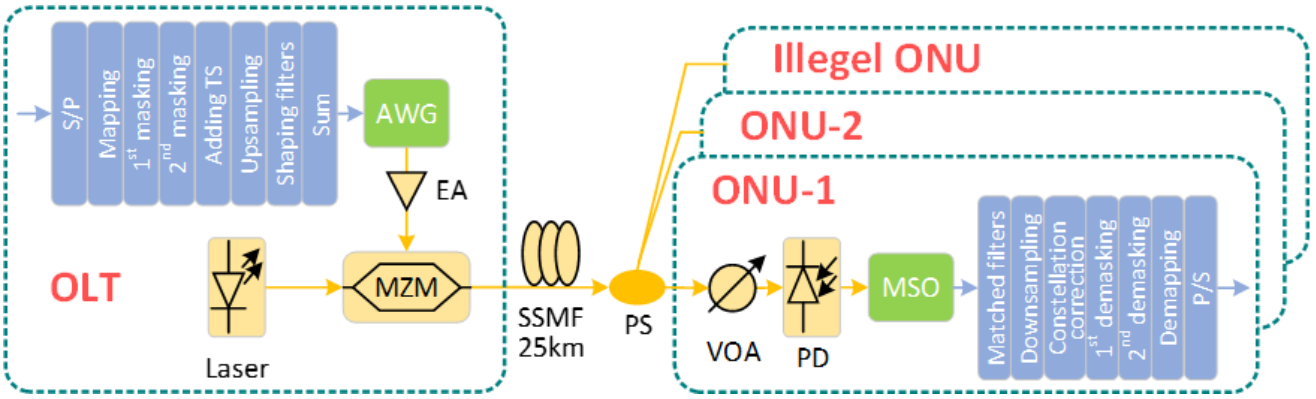

FIGURE 5. Experimental setup (AWG: arbitrary waveform generator; EA: electrical amplifier; MZM: Mach-Zehnder modulator; PS: power splitter; VOA: variable optical attenuator; PD: photodiode; MSO: mixed signal oscilloscope).

3D-CAP signal by a mixed signal oscilloscope (MSO) with sampling rate of 50 GSa/s, offline DSP, which is reverse to that at the OLT, can perform decrypting function to recover the original data.

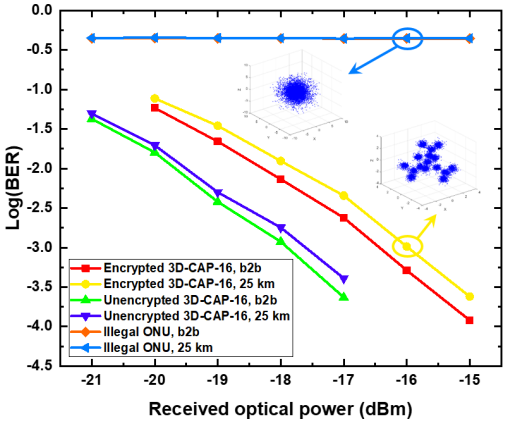

FIGURE 6. BER curves of encrypted 3D-CAP-16, unencrypted 3D-CAP-16, and illegal ONU for b2b and 25 km transmission (b2b: back to back).

Figure 6 illustrates the BER curves of encrypted 3D-CAP-16, unencrypted 3D-CAP-16, and illegal ONU before and after 25 km transmission. In the experiment, legal ONU is given the correct key in terms of initial values, control parameters and step lengths of the chaotic models, which the illegal one is not aware of (i.e., incorrect key). The baud rate is set as 1 Gbaud, and the corresponding bit rate is 4 Gb/s. It can be seen that due to the increased constellation chaos by the constellation masking, the power penalty after 25 km transmission is about 0.45 dB for the encrypted 3D-CAP-16 signal, while the unencrypted 3D-CAP-16 signal without constellation masking displays a smaller power penalty of about 0.3 dB. Compared with the unencrypted 3D-CAP-16 signal, the encrypted 3D-CAP-16 signal has a receiver sensitivity penalty of 1.6 dB after 25 km transmission at a BER of 1×10^{-3}. However, the security performance of the proposed encryption scheme is very impressive. As the received optical power increases, the BER performance of the legal ONU is more favorable, while the illegal one consistently maintain the BER of about 0.45. It is obvious seen that without the correct key, illegal ONU can't acquire any information destined for legal ONU. Moreover, the received constellations of legal ONU and illegal one are also shown in Fig. 6. Contrary to the clear 3D constellation for the legal ONU, what the illegal one obtain is a dense and disordered sphere with few recognition of the original 3D constellation.

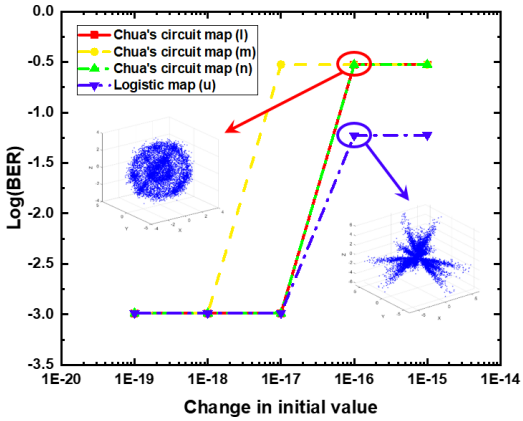

FIGURE 7. BER curves of various ONUs with a tiny change in initial value.

In a bid to verify the sensitivity to the initial values of the chaotic models, as well as the security of data encryption, Fig. 7 shows the BER curves of various ONUs with a tiny change in initial value after 25 km transmission when the received optical power is −16 dBm. The initial values $\{l_0, m_0, n_0, u_0\}$ of the chaotic models are set as {0.2, −0.1, 0.2, 0.37259}. As can be seen in Fig. 7, as the initial value slightly changes, such as $\{0.2+10^{-16}, -0.1, 0.2, 0.37259\}$, $\{0.2, -0.1+10^{-17}, 0.2, 0.37259\}$, $\{0.2, -0.1, 0.2+10^{-16}, 0.37259\}$, or $\{0.2, -0.1, 0.2, 0.37259+10^{-16}\}$, dramatic increase can be observed in terms of BER. And a tiny change of 10^{-16} for the initial values of l or n, or 10^{-17} for m, can raise the BER to about 0.3, in which case the illegal ONU is unable to eavesdrop on the encrypted data transmission. As for a tiny change of 10^{-16} for the initial value of u, since

only scaling-based constellation masking with factor of 1∼3 is performed in absence of constellation rotation, BER can only be increased to 0.06, which is also above the forward error correction (FEC) threshold. In addition, the corresponding constellation are also shown as the insets in Fig. 7.

Furthermore, the key space of the proposed encryption scheme is calculated and evaluated in a conservative manner. The secret key includes the initial values, control parameters and step lengths of both Chua's circuit map and Logistic map, namely $\{l_0, m_0, n_0, u_0, a,\ b, c, d, \lambda, t_1,\ t_2\}$. Normally the control parameters of the chaotic models are set to typical values, making it effortless for the illegals to tap into, so in this paper the key space is assessed conservatively with only initial values and step lengths being taken into consideration. If the range of step lengths is [1, 10^3], the key space can be deduced as $(6\times10^{16})\times(2\times10^{17})\times(10\times10^{16})\times(1\times10^{16})\times 10^3\times 10^3 = 1.2\times10^{73}$. Such enormous is the key space that searching for the correct key can be way too time-consuming, thus effectively guarding against those brute force attacks trying to obtain the right key.

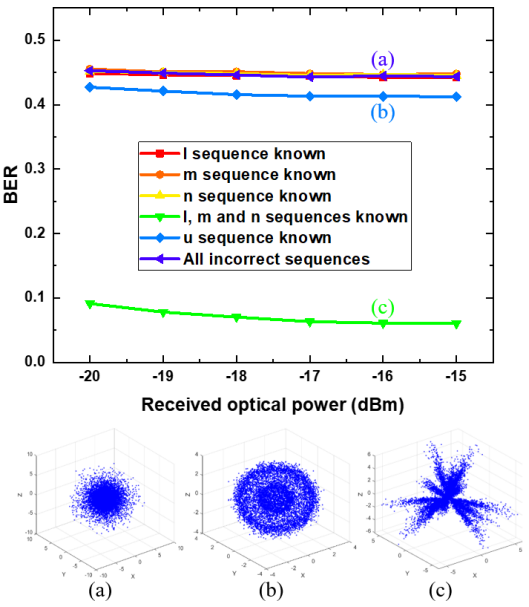

FIGURE 8. BER curves of an illegal ONU under all possible conditions.

In this paper, both first-stage masking based on constellation rotation and second-stage one based on constellation scaling are carried out, where rotation is determined by chaotic sequences of $\{l, m, n\}$, while scaling by chaotic sequence of u. Figure 8 depicts the BER curves of an illegal ONU in the condition of different known sequences after 25 km transmission. It can be seen that BER is about 0.45 when all the chaotic sequences remain unknown. While only l, m or n is given, BER also keeps at around 0.45. At this moment, as can be seen in Fig. 8(a), constellation is taking on a dense and disordered sphere, leaving the illegal ONU unable to recover the whereabouts of the original constellation. This can be attributed to the constellation masking based on rotation and scaling. When the chaotic sequence of u is known, only rotating-based constellation masking is implemented, leaving the constellation present as two spherical layers with different radii, as shown in Fig. 8(b). The BER is about 0.42 at this moment, slightly below the one in the case of all unknown sequences, while far more above the FEC threshold. When the chaotic sequences of $\{l, m, n\}$ all remain known, only scaling-based constellation masking is functioning, bringing about the radial-like constellation as shown in Fig. 8(c). As the scaling factor is strictly restricted in the range of 1∼3, BER keeps at a rather low level of 0.06, also above the FEC threshold, which enables the system robustness against illegal ONU attacks. Experimental results indicate that the proposed scheme is sensitive to all kinds of chaotic sequences, thus guaranteeing the secure encrypted transmission without any information leaking.

IV. CONCLUSION

We have proposed a security-enhanced 3D-CAP-PON based on two-stage spherical constellation masking, where Chua's circuit map and one-dimensional Logistic map are applied to implement rotating-based and scaling-based 3D-constellation masking, respectively. Taking the dimension into higher level, 3D-constellation masking enables more flexibility and effectively enhances the security of the encryption scheme through the combination of two joint chaotic models. Conservative evaluation shows that the key space of the proposed encryption scheme is 1.2×10^{73} when not taking control parameters into consideration, making it almost impossible for hacking from the illegal ONU. Moreover, the feasibility of the proposed scheme is verified by a 4 Gb/s encrypted 3D-CAP-16 signal transmission over 25 km SSMF. Experimental results suggest that the proposed scheme could be an effective solution for future secure physical-layer communication in 3D-CAP-PON.

REFERENCES

[1] J. Zhang, J. Yu, X. Li, K. Wang, W. Zhou, J. Xiao, L. Zhao, X. Pan, B. Liu, and X. Xin, "200 Gbit/s/λ PDM-PAM-4 PON system based on intensity modulation and coherent detection," *J. Opt. Commun. Netw.*, vol. 12, no. 1, pp. A1–A8, Jan. 2020.

[2] X. Xu, B. Liu, X. Wu, L. Zhang, Y. Mao, J. Ren, Y. Zhang, L. Jiang, and X. Xin, "A robust probabilistic shaping PON based on symbol-level labeling and rhombus-shaped modulation," *Opt. Express*, vol. 26, no. 20, pp. 26576–26589, 2018.

[3] A. Mikaeil, W. Hu, T. Ye, and S. B. Hussain, "Performance evaluation of XG-PON based mobile front-haul transport in cloud-RAN architecture," *IEEE/OSA J. Opt. Commun. Netw.*, vol. 9, no. 11, pp. 984–994, Nov. 2017.

[4] Y. Luo, H. Roberts, K. Grobe, M. Valvo, D. Nesset, K. Asaka, H. Rohde, J. Smith, J. S. Wey, and F. Effenberger, "Physical layer aspects of NG-PON2 standards—Part 2: System design and technology feasibility," *J. Opt. Commun. Netw.*, vol. 8, no. 1, pp. 43–52, Jan. 2016.

[5] L. Sun, J. Du, and Z. He, "Multiband three-dimensional carrierless amplitude phase modulation for short reach optical communications," *J. Lightw. Technol.*, vol. 34, no. 13, pp. 3103–3109, Jul. 1, 2016.

[6] L. Sun, J. Du, Y. You, C. Liang, W. Zhang, L. Ma, and Z. He, "45-gbps 3D-CAP transmission over a 16-GHz bandwidth SSMF link assisted by Wiener filtering," *Opt. Commun.*, vol. 389, pp. 118–122, Apr. 2017.

[7] J. Ren, B. Liu, X. Wu, L. Zhang, Y. Mao, X. Xu, Y. Zhang, L. Jiang, J. Zhang, and X. Xin, "Three-dimensional probabilistically shaped CAP modulation based on constellation design using regular tetrahedron cells," *J. Lightw. Technol.*, vol. 38, no. 7, pp. 1728–1734, Apr. 1, 2020.

[8] J. Zhang, J. Yu, F. Li, N. Chi, Z. Dong, and X. Li, "11×5×9.3Gb/s WDM-CAP-PON based on optical single-side band multi-level multi-band carrier-less amplitude and phase modulation with direct detection," *Opt. Express*, vol. 21, no. 16, pp. 18842–18848, Aug. 2013.
[9] J. Ren, B. Liu, X. Xu, L. Zhang, Y. Mao, X. Wu, Y. Zhang, L. Jiang, and X. Xin, "A probabilistically shaped star-CAP-16/32 modulation based on constellation design with honeycomb-like decision regions," *Opt. Express*, vol. 27, no. 3, pp. 2732–2746, Feb. 2019.
[10] L. Zhang, X. Xin, B. Liu, and Y. Wang, "Secure OFDM-PON based on chaos scrambling," *IEEE Photon. Technol. Lett.*, vol. 23, no. 14, pp. 998–1000, Jul. 2011.
[11] M. Bi, X. Fu, X. Zhou, L. Zhang, G. Yang, X. Yang, S. Xiao, and W. Hu, "A key space enhanced chaotic encryption scheme for physical layer security in OFDM-PON," *IEEE Photon. J.*, vol. 9, no. 1, Feb. 2017, Art. no. 7901510.
[12] W. Zhang, C. Zhang, C. Chen, H. Zhang, W. Jin, and K. Qiu, "Hybrid chaotic confusion and diffusion for physical layer security in OFDM-PON," *IEEE Photon. J.*, vol. 9, no. 2, Apr. 2017, Art. no. 7201010.
[13] L. Zhang, B. Liu, X. Xin, and Y. Wang, "Joint robustness security in optical OFDM access system with Turbo-coded subcarrier rotation," *Opt. Express*, vol. 23, no. 1, pp. 13–18, Jan. 2015.
[14] B. Liu, L. Zhang, X. Xin, and J. Yu, "Constellation-masked secure communication technique for OFDM-PON," *Opt. Express*, vol. 20, no. 22, pp. 25161–25168, Oct. 2012.
[15] L. Zhang, B. Liu, X. Xin, and D. Liu, "A novel 3D constellation-masked method for physical security in hierarchical OFDMA system," *Opt. Express*, vol. 21, no. 13, pp. 15627–15633, Jul. 2013.
[16] W. Zhang, C. Zhang, C. Chen, and K. Qiu, "Experimental demonstration of security-enhanced OFDMA-PON using chaotic constellation transformation and pilot-aided secure key agreement," *J. Lightw. Technol.*, vol. 35, no. 9, pp. 1524–1530, May 1, 2017.
[17] J. Zhong, X. Yang, and W. Hu, "Performance-improved secure OFDM transmission using chaotic active constellation extension," *IEEE Photon. Technol. Lett.*, vol. 29, no. 12, pp. 991–994, Jun. 15, 2017.
[18] A. Sultan, X. Yang, A. A. E. Hajomer, and W. Hu, "Chaotic constellation mapping for physical-layer data encryption in OFDM-PON," *IEEE Photon. Technol. Lett.*, vol. 30, no. 4, pp. 339–342, Feb. 15, 2018.
[19] P. Shi, H. Huan, and R. Tao, "Waveform design for higher-level 3D constellation mappings and its construction based on regular tetrahedron cells," *Sci. China Inf. Sci.*, vol. 58, no. 8, pp. 1–12, Aug. 2015.
[20] L. O. Chua, M. Komuro, and T. Matsumoto, "The double scroll family," *IEEE Trans. Circuits Syst.*, vol. 33, no. 11, pp. 1072–1118, Nov. 1986.
[21] S.-L. Che, T. Hwang, and W.-W. Lin, "Randomness enhancement using digitalized modified logistic map," *IEEE Trans. Circuits Syst. II, Exp. Briefs*, vol. 57, no. 12, pp. 996–1000, Dec. 2010.

JIANXIN REN received the B.S. degree in electronic science and technology from the Beijing University of Chemical Technology (BUCT), Beijing, China, in 2016. He is currently pursuing the Ph.D. degree in optical engineering with the State Key Laboratory of Information Photonics and Optical Communications, Beijing University of Posts and Telecommunications (BUPT), China. His research interests include optical communication, passive optical networks, and optoelectronics.

BO LIU received the bachelor's and Ph.D. degrees in optical engineering from the Beijing University of Posts and Telecommunications, Beijing, China, in 2008 and 2013, respectively. He is currently a Professor with the School of Physics and Optoelectronics, NUIST, China. His research interests include all optical signal processing, radio over fiber, and broadband optical communication.

XIANGYU WU received the B.S. degree in electronic engineering from BUPT, China, in 2015, where he is currently pursuing the Ph.D. degree in electronic science and technology with the State Key Laboratory of Information Photonics and Optical Communications. His research interests include optical communication systems, optical inter-connects, and integration network technology.

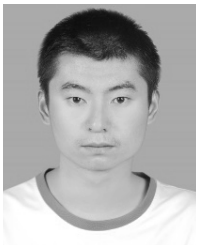

XING XU received the B.S. degree from the Beijing University of Posts and Telecommunications, China, in 2015, where he is currently pursuing the Ph.D. degree in electrical science and technology. His research interests include optical access networks and SDN architecture.

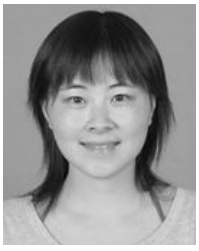

YAYA MAO received the bachelor's degree from Nanjing Normal University, in 2003, and the Ph.D. degree from Beijing Jiaotong University, in 2017. She is currently an Associate Professor with the Institute of Optoelectronics Research, NUIST, China. Her current research interests include optical communication and all signal processing.

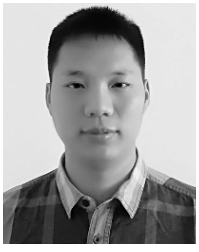

YONGFENG WU received the Ph.D. degree in physical electronics from the Harbin Institute of Technology (HIT), China, in 2018. He is currently an Associate Professor with the Institute of Optics and Electronics, Nanjing University of Information Science and Technology (NUIST), China. His current research interest includes optical fiber sensors.

XIUMIN SONG received the B.S. degree from Shandong Agricultural University, China, in 2017. She is currently pursuing the Ph.D. degree in electrical science and technology with the Beijing University of Posts and Telecommunications. Her research interests include optical communication systems and novel optical fiber.

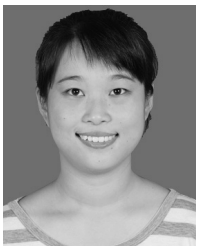

LEI JIANG received the bachelor's degree in applied physics from the Nanjing University of Information Science and Technology (NUIST), China, in 2017, where she is currently pursuing the master's degree with the School of Physics and Optoelectronics. Her research interests include optical communication, passive optical networks, and optical signal processing.

JINGYI ZHANG received the bachelor's degree in communication engineering from Hangzhou Dianzi University, China, in 2018. She is currently pursuing the master's degree in physics and optoelectronics with NUIST, China. Her research interests include optical communication, passive optical networks, and optical signal processing.

YING ZHANG received the B.S. degree in electronic science and technology from the Beijing University of Chemical Technology, Beijing, China, in 2014, and the Ph.D. degree in optical engineering from the Beijing University of Posts and Telecommunications, Beijing, in 2019. She is currently a Postdoctoral Researcher with the Department of Electronics, School of Electronics Engineering and Computer Science, Peking University, Beijing. Her research interests include optical communication, optical signal processing, radio over fiber, passive optical networks, and optoelectronics.

XIANGJUN XIN received the Ph.D. degree in electromagnetic field and microwave technology from the Beijing University of Posts and Telecommunication (BUPT), Beijing, China, in 2004. He is currently a Professor with the School of Electronic Engineering and a member with the State Key Laboratory of Information Photonics and Optical Communications, BUPT. He has more than 100 publications in prestigious journals and conferences. His main research interests include high-speed fiber communication systems, broadband optical transmission technologies, and all-optical networks.